Systems & Control Transactions

Research Article - Peer Reviewed Conference Proceeding
ESCAPE 35 - European Symposium on Computer Aided Process Engineering
Ghent, Belgium. 6-9 July 2025
Jan F.M. Van Impe, Grégoire Léonard, Satyajeet S. Bhonsale,
Monika E. Polańska, Filip Logist (Eds.)

PSE PRESS

Optimal Hydrogen Flux in a Catalytic Membrane Water Gas Shift Reactor

Nabeel S. Abo-Ghander[a], Filip Logist[b]

[a] Department of Chemical Engineering, Interdisciplinary Center for Refining & Advanced Chemicals, King Fahd University of Petroleum & Minerals, Dhahran 31261, Saudi Arabia.
[b] BioTeC+, Department of Chemical Engineering, KULeuven, Gebroeders de Smetstraat 1, 9000 Ghent, Belgium.
* Corresponding Author: naboghander@gmail.com.

ABSTRACT

A one-dimensional homogeneous reactor model for a cocurrent flow nonadiabatic catalytic membrane reactor operating water gas shift reaction (WGSR) is developed. The model is used to predict the performance of the reactor and estimate the optimal hydrogen flux profiles required to maximize the CO conversion, and control the temperature rise due to the exothermicity. Under the optimized condition, the secured optimal hydrogen flux is found to be a bang-bang type suggesting constructing reactors of different hydrogen permeabilities. To control the reactor temperature, the activity of the reaction side is diluted by distributing axially certain fractions of inert solid, i.e. 0.35, 0.45 and 0.50. The total volume fraction of the inert solid required to maintain the temperature at 320°C (593.15 K) is 0.50 and the profile is obtained to be a singular-arc type with an observed maximum activity at the reactor inlet.

Keywords: Modelling, Optimization, Reaction Engineering, Simulation, Membranes, water gas shift reaction, membrane reactor, bang-bang controller, singular-arc controller, optimal hydrogen flux, inert solid distribution

INTRODUCTION

Hydrogen is considered to be a potential future replacement for fossil fuel [1]. It is produced industrially by steam reforming of hydrocarbons or water gas shift reaction. Both processes are thermodynamically-limited whose conversion is favored by operating the reactions in nonconventional catalytic reactors such as membrane reactors. In membrane reactors, the H_2 production can be boosted via in-situ separation which takes place when hydrogen permeative membranes are installed. Two main types of catalysts have been developed over the years for the water gas shift reaction. The first one, which has been used for many years, is an iron–based catalyst on which CO is oxidized in the presence of steam to hydrogen and CO_2 at a temperature range of 350–500°C [2]. This catalyst is known to be a high-temperature water gas shift reaction catalyst. The second one is a copper-based catalyst on which the reaction is operated at a temperature range of 150-250°C, and the catalyst is referred to as a low-temperature water gas shift reaction catalyst [3]. For these two types of catalysts, various mathematical reaction rate expressions were developed based on power-law kinetic models, Eley–Rideal, and Langmuir–Hinshelwood kinetic models [4]. An excellent review with a summary of different kinetic models is given by Saeidi et al [5] and Shahid et al [1].

As far as the reactor modelling is concerned, numerous mathematical models were proposed for the water gas shift reactor accounting for the changes in molar flowrates of species, reactor temperature and pressure with different degrees of sophistication [6-8]. Those models were used to conduct parameter sensitivity analysis, predictions, and optimization of reactor performance.

In this work, the theory of optimal control is applied to a cocurrent flow nonadiabatic catalytic membrane WGSR to optimally design for suitable hydrogen fluxes required to maximize the CO conversion and controlling the temperature inside this reactor. This problem has not been yet addressed in the literature for membrane reactors and the results presented in this study can greatly assist in providing rigorous decisions about the proper set-up of the reactor configurations required to achieve the set goals.

KINETICS AND REACTION RATE LAW

Water gas shift reaction is described by the following stoichiometric equation:

$$CO + H_2O \Leftrightarrow H_2 + CO_2 \; \Delta H^0_{298} = -41.1 \frac{kJ}{mol} \quad [1]$$

The reaction is moderately exothermic, reversible, and its conversion can be favored by operating at low temperatures in conversional fixed bed reactors. The kinetic expression of the water gas shift reaction expressed in mol/ (kg cat ×s) on a commercial Cu/ZnO/AlO_3 catalyst is given in terms of the component partial pressure as follows [9,10]:

$$r = 82.4 \times 10^3 \, exp\left(-\frac{47400}{RT}\right)\left[p_{CO}p_{H_2O} - \frac{p_{H_2}p_{CO_2}}{K_{eq}}\right] \quad [2]$$

The equilibrium constant can be estimated using:

$$K_{eq} = exp\left(\frac{4577.8}{T} - 4.33\right) \quad [3]$$

REACTOR CONFIGURATION

The co-current configuration of the catalytic membrane water gas shift reactor utilized in this study is depicted in Figure 1. The reactor is composed of two main concentric tubes separated by a highly selective hydrogen permeative membrane wall extending along the axial distance of the reactor.

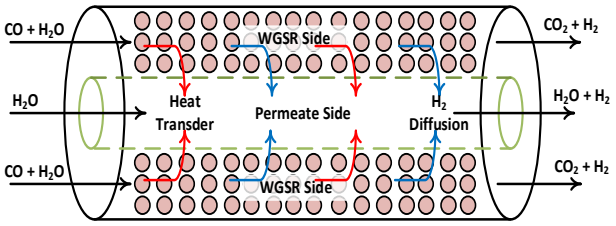

Figure 1: Co-current configuration of the catalytic membrane water gas shift reactor.

On the outer side, a copper-based catalyst is used to pack the bed allowing low-temperature water gas shift reaction to take place. The feed to this side is mainly composed of carbon monoxide, steam and inert gases introduced at a temperature of 200°C and a pressure of 1.5 atm. While the reaction takes place in the outer tube, both hydrogen and heat are produced, and exchanged with the permeate side.

On the inner side, pure steam at a temperature of 120°C is introduced. It is used to create an appreciable driving force along the membrane reactor and purge the diffused hydrogen out of the reactor.

REACTOR MATHEMATICAL MODELLING

The reactor model equations are derived considering the assumptions of steady-state operation of both sides of the reactor, ideal gas behavior, plug-flow reactor model, negligible effect of the catalyst deactivation, adiabatic reactor external wall, negligible diffusional resistances, highly selective hydrogen permeative membranes are installed, the pressure drop on the reaction side is estimated using Ergun's equation, and negligible pressure drop on the permeate side. The governing equations of the reactor are given as:

Mole balance:

$$\frac{dn_i}{dz} = \sigma_i r \rho_s (1-\varepsilon)(1-u_1)A_c - 2\pi R_3 \psi_i u_2 \quad [4]$$

Energy balance:

$$\frac{dT}{dz} = \frac{[-\Delta H(T)]r\rho_s(1-\varepsilon)(1-u_1)A_c - 2\pi R_3 U(T-T') - \sum_{i=1}^{n} 2\pi R_3 \psi_i u_2 \int_{T'}^{T} C_{pi} dT}{\sum_{i=1}^{n} n_i C_{pi}} \quad [5]$$

Pressure drop:

$$\frac{dP}{dz} = -\frac{G}{\rho D_p g_c}\left(\frac{1-\varepsilon}{\varepsilon^3}\right)\left[\frac{150\mu(1-\varepsilon)}{D_p} + 1.75G\right] \quad [6]$$

On the permeate side, the equations are given by:

$$\frac{dn_i'}{dz} = 2\pi R_3 u_2 \quad [7]$$

$$\frac{dT'}{dz} = \frac{2\pi R_3 U(T-T') + \sum_{i=1}^{n} 2\pi R_3 \psi_i u_2 \int_{T'}^{T} C_{pi} dT}{\sum_{i=1}^{n} n_i' C_{pi}'} \quad [8]$$

The boundary conditions are defined at the reactor inlet for the cocurrent configuration as follows:

At $z = 0$:

$$n_i = n_{i0} \qquad T = T_0 \qquad P = P_0 \quad [9]$$

$$n_i' = n_{i0}' \qquad T' = T_0' \quad [10]$$

In the above reactor model equations, two control variables are included, namely the inert solid volume fraction u_1 and hydrogen flux u_2. The volume inert solid fraction is a dimensionless variable defined as the ratio of the volume of the inert solid to the total solid fraction present on the reaction side, while the hydrogen flux is defined as moles of hydrogen exchanged per unit time per unit surface area. Both variables are determined numerically based on prescribed performance measures. Additionally, the phi parameter ψ_i introduced in the model equations owns a value of one for hydrogen and zero otherwise. The overall heat transfer coefficient U between the reaction side and permeate side is estimated using a composite wall correlation.

MATHEMATICAL FORMULATION OF THE OPTIMIZATION PROBLEMS

The optimization problems can be stated as follows:

Let $U_1$and U_2 be the set of all admissible profiles of solid volume fraction and hydrogen flux, respectively.

The optimization problems encountered in this study is to compute $u_1(z) \in U_1$ and/or $u_2(z) \in U_2$ such that a performance measure is minimized without violating the governing model equations of the catalytic membrane WGSR and/or any other specified equality or inequality constraints.

Three objective functions are considered in this study for the membrane catalytic reactor and defined as conversion of carbon monoxide achieved in the reaction side, temperature cost at the reactor exit, and variation cost of the temperature inside the reactor with respect to a set temperature, i.e. 320°C. The mathematical representation is given as:

$$J_1(x,u_1,u_2) = \frac{n_{CO}^f - n_{CO}}{n_{CO}^f} \quad [11]$$

$$J_2(x,u_1,u_2) = [T(L) - T_R]^2$$

$$[12] J_3(x,u_1,u_2) = [T(L) - T_R]^2 + \int_0^L (T - T_R)^2 dz \quad [13]$$

The mathematical formulation of the optimization problem can be stated as follows:

$$\underset{x,u_1,u_2}{Min}\ J_i(x,u_1,u_2) \qquad i \in \{1,2,3\} \quad [14]$$

Subject to:

$$F(x,u_1,u_2) = 0 \quad [15]$$

The conversion of carbon monoxide is multiplied by "-1" to convert the maximization problem to minimization in Eq [11]. Eq [15] is a vector representing the conservation nonlinear algebraic equations of the reactor model equations obtained by discretizing the ordinary differential equations using Hermite-Simpson collocation technique.

The hydrogen flux along the WGSR expressed in mol/(m^2×s) is the main optimal profile to be determined. The bound is set to be:

$$0.5 \le u_2 \le 8.0 \quad [16]$$

The hydrogen recovery defined as cumulative molar flowrate of hydrogen diffused to the permeate side with respect to CO fed to the reactor is controlled by setting a hard constraint given by the following nonlinear algebraic equation:

$$n'_{H_2}(L) - n^R_{H_2} = 0 \quad [17]$$

The hydrogen recovery is varied in this study between two limits, i.e. 1.25 and 1.75 mol/s.

The inert solid volume fraction is introduced to the optimization problems in order to control the temperature inside the reactor. The total volume fraction of the inert solid is defined along the dimensionless axial distance as:

$$\bar{u}_1 = \int_0^{1.0} u_1(\zeta) d\zeta \quad [18]$$

The total volume fraction of the inert solid is varied assuming the values of 0.35, 0.45 and 0.50 and the bound on the solid volume fraction is given by:

$$0.0 \le u_1 \le 1.0 \quad [19]$$

A summary of the optimization problem addressed in this work and the reactor design and operational parameters are given in Tables 1 and 2, respectively. The optimization problems are solved numerically using SNOPT.

Table 1: Optimization problem set-up

Problem	Case No.	Objective function	Control variables	H_2 recovery constraints
1	1	$J = J_1$	H_2 flux	NA
	2	$J = 0.01J_1 + 0.99J_2$	H_2 flux	NA
	3	$J = J_2 + J_3$	H_2flux	NA
2	1	$J = J_1$	H_2 flux	1.25 mol/s
	2	$J = J_1$	H_2 flux	1.75 mol/s
3	1	$J = J_2 + J_3$	H_2 flux & inert volume fraction	NA

Table 2: Reactor design and operating parameters

Parameter	Numerical value	Unit
Reactor length	3.0	m
Reactor inner radius	0.05	m
Stainless steel thickness	2.0×10^{-3}	m
Membrane thickness	1.0×10^{-6}	m
Reactor outer radius	0.08	m
Diameter of catalyst particles	6.0×10^{-3}	m
Catalyst density	2500	Kg/m^3
Bed porosity	0.55	--
Reaction Side		
Feed molar flowrate	5.0	mol/s
Feed composition		
CO	0.2749	--
H_2O	0.3165	--
CO_2	0.1198	--
H_2	0.2686	--
N_2	0.0202	--
Feed temperature	473.15	K
Feed pressure	1.5	atm
Permeate side		
Steam molar flowrate	25.0	mol/s
Steam feed temperature	393.15	K
Steam feed pressure	1.0	atm

Without catalyst dilution

For the first optimization problem, the objective functions considered were the conversion of CO in the reactor, a linear combination of the conversion of CO and

the exit temperature cost with a weight of 0.99 and 0.01, and a temperature cost combining the temperature inside the reactor and at the exit point. The optimization problems were solved for the optimal H_2 flux profiles with no constraints on the H_2 recovery.

In Figure 2, the conversion of carbon monoxide and the equilibrium conversion are plotted against the dimensionless axial distance for all scenarios. It is observed that the CO conversion inside the membrane reactor is higher than those of the equilibrium due to the hydrogen permeation. The maximum conversion observed is when the objective function is the conversion of CO, while the second highest is observed when the temperature of the reactor is controlled inside the reactor and at the exit. The reduction in CO conversion in the reactor when the temperature is controlled, is due to the low H_2 recovery, i.e. less H_2 diffused from the reaction side to the permeate side. In all three optimization scenarios, the estimated reactor conversions are >~ 95%.

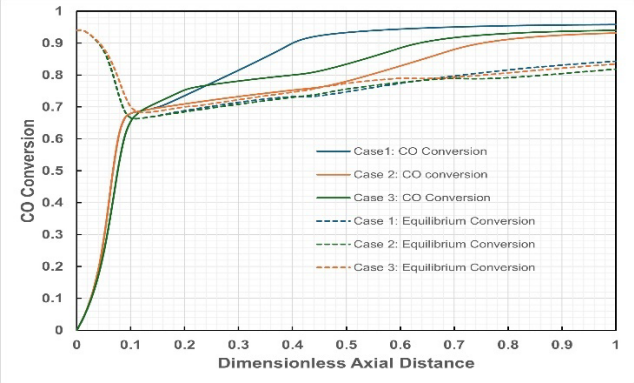

Figure 2: CO conversion and equilibrium conversion profiles for the cases of maximizing CO conversion, minimizing exit and reactor temperature.

The optimal hydrogen flux profiles expressed in mole/(m^2×s) are plotted vs. the dimensionless reactor distance in Figure 3 for all optimization problems.

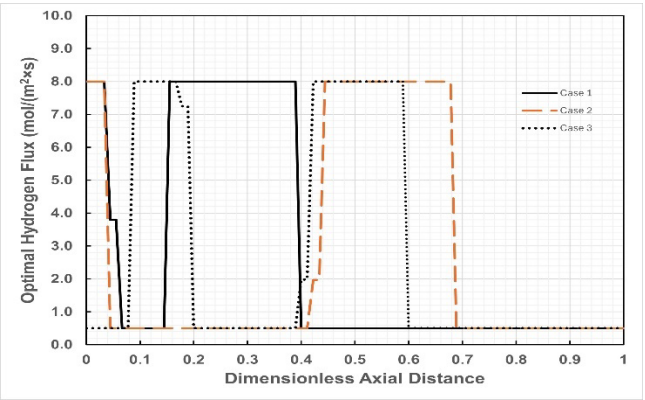

Figure 3: Optimal H_2 flux profiles based on maximizing CO conversion, minimizing exit and reactor temperature.

All the three control profiles computed are **bang-bang** type with no singular intervals due to the fact that the Hamiltonian for the reactor depends affinely on the hydrogen flux. The hydrogen flux alternates between 8.0 mole/ (m^2×s) and 0.5 mole/ (m^2×s) representing two types of membrane reactors with high and low H_2 permeation rates achieved by the installation of H_2 membranes with different fluxes. To maximize the conversion of CO, it is observed that maximum hydrogen flux is required at the reactor inlet, while minimum hydrogen flux is required when the reactor temperature is to be controlled. At the reactor outlet, a low hydrogen flux is required as the conversion of CO approaches completion.

In Figure 4, the temperature profiles on the reaction side are plotted along the dimensionless axial distance. The reactor temperature increases due to the reaction, then decreases due to heat exchange with the permeate side. For a set temperature of 320°C (593.15K), It is observed that the maximum deviation is depicted when the CO conversion is maximized. However, this deviation decreases as the objective function is redefined to include the temperature deviation terms in cases 2 and 3.

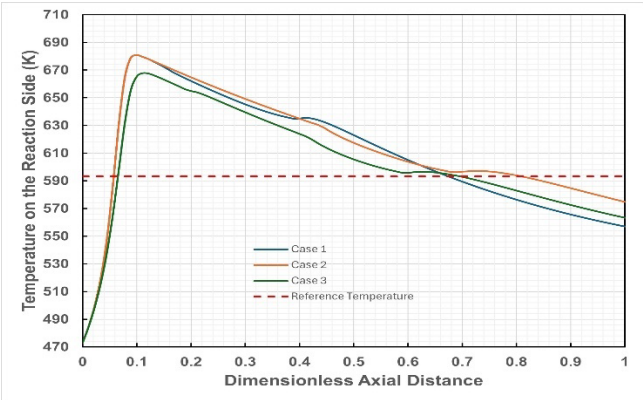

Figure 4: Temperature profiles based on maximizing the CO conversion, minimizing exit and reactor temperature.

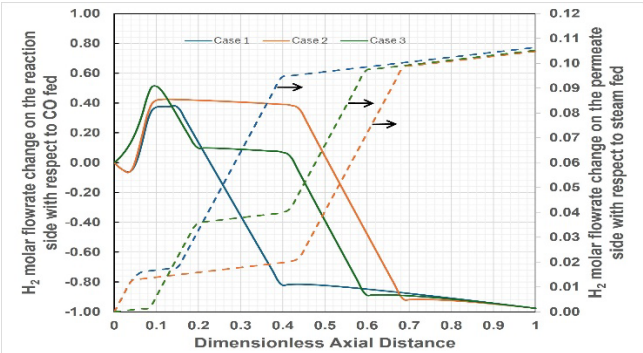

Figure 5: Change in H_2 molar flowrate profiles on the reaction side and permeate.

The fractional change of the molar flowrates of hydrogen on the reaction side and the permeate side are plotted against the dimensionless distance in Figure 5.

On the reaction side, the molar flowrate of hydrogen decreases within the fractional length of ~0.05 due to the maximum hydrogen flux of 8.0 mol/(m^2×s) for the case of maximizing the CO conversion, increases due to production by the reaction, then decreases due to the diffusion. When reactor temperature is controlled, hydrogen is maintained inside the reaction side as much as possible as this suppresses the progress of the reaction. On the permeate side of the reactor, it is observed that the sharpest and fastest change is obtained when the CO is maximized where most of hydrogen is recovered within 0.40 fractional length.

In Figure 6, the conversion of CO is plotted along the dimensionless axial distance for unlimited hydrrogen recovrery, 1.25 mol/s, and 1.75 mol/ s. In all cases, the conversion of the carbon monoxide increases along the reactor with a significant difference for the case where the H_2 recovery is maximum, i.e. no constraint is set on H_2 recovery.

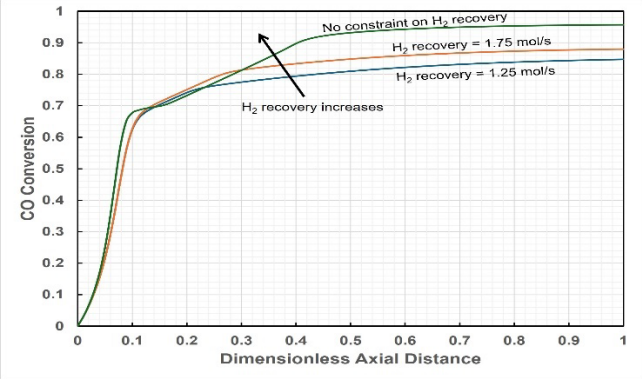

Figure 6: Influence of H_2 recovery on the CO conversion.

In Figure 7, the molar flowrate of diffused H_2 on the permeate side is plotted against the dimensionless axial distance.

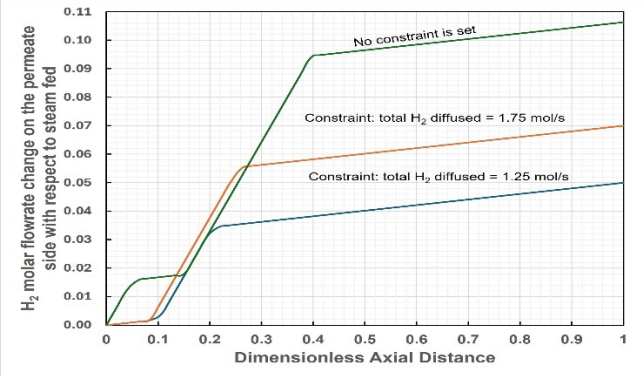

Figure 7: Influence of hydrogen recovery on hydrogen flowrate on the permeate side.

All curves show that H_2 molar flowrate increases inside the permeate side due to the flux through the membrane but the one with no H_2 flux limitation gives the highest H_2 recovery in the membrane reactor.

With catalyst dilution

To control the temperature inside the reactor so that it does not exceed 320°C (593.15K), an inert solid is axially distributed. The distribution profiles of the inert solid for total average amounts of 0.35, 0.45 and 0.50, and the corresponding CO conversion profiles are shown in Figure 8.

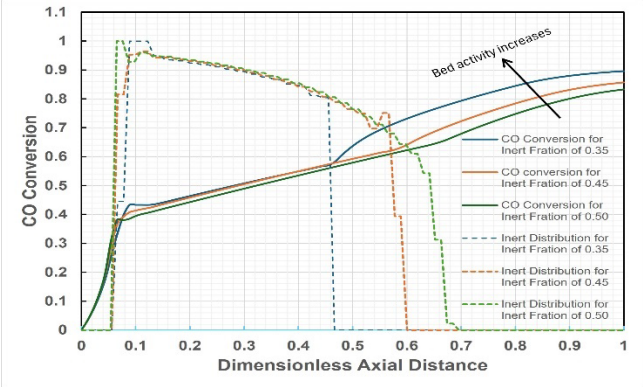

Figure 8: Optimal solid inert distribution and the corresponding CO conversion profiles.

At the reactor entrance, it is required to have the catalytic bed fully active indicated by zero inert solid volume fraction. This causes a ramp in the reactor temperature from the feed temperature to the required set temperature as shown in Figure 9.

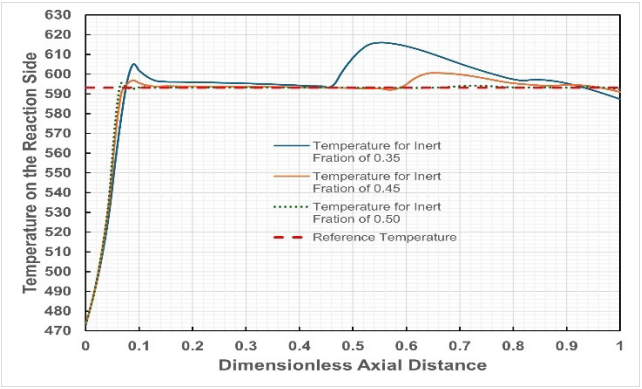

Figure 9: Temperature profiles for total inert solid fraction of 0.35, 0.45 and 0.50.

A peak is then formed at which the bed is made to be inactive by setting the volume fraction of the inert solid to unity. This causes the generated reaction heat rate to be zero and only heat exchange between the reaction side and the permeate side takes place. After that, a decreasing inert solid fraction profile is utilized to adjust the temperature to get close to 320°C. The average solid volume fraction of 0.35 gives the highest temperature

deviation compared to the other two scenarios of 0.45 and 0.50 as most of the inert solid is used to reduce the temperature in the reaction side and none is left to maintain the temperature close to 320°C. The optimal inert solid distribution profiles on the reaction side are a **min-max-singular-min** types recommending the utilization of a catalytic membrane reactor with four activity zones, i.e. fully active bed followed by an inactive bed followed by a mixed catalyst bed and finally an active bed.

CONCLUSION

A 1D homogeneous steady-state reactor model for a membrane catalytic water gas shift reactor was developed. The model was used to secure the optimal H_2 flux required to maximize the yield conversion and controlling the temperature along the reactor axial distance. In addition, the reactor model was used to optimize the distribution of the inert solid required to maintain the temperature of the reactor not exceeding 320°C (593.15K) and eliminating the hot spot formed due to the reaction exothermicity. The maximization of CO conversion requires hydrogen flux to be maximum at the reactor entrance as this shift the thermodynamic equilibrium and achieving higher conversion. The scenario was the opposite when the temperature is to be controlled where minimum hydrogen flux is needed at the reactor entrance so that the reaction progress is suppressed and amount of heat released is minimized, too. The hydrogen optimal flux profile is a bang-bang controller type with five switching points indicating that membrane reactors with different permeability must be used. The inert solid distribution used to control the temperature inside the reactor shows that a singular arc must be implemented where a fully active bed has to be used at the entrance to favor the temperature rise to the set temperature.

ACKNOWLEDGEMENTS

The Author would like to acknowledge Interdisciplinary Research Center for Refining and Advanced Chemicals, King Fahd University of Petroleum & Minerals, Dhahran, Saudi Arabia for the financial support for this work through Project # INRC2319.

NOMENCLATURE

A_c: cross-sectional area of the reaction side, [m2].
C_{pi}: heat capacity of species i (reaction side), [J/(mol×K)].
$C_{pi}^{'}$: heat capacity of species i (permeate side), [J/(mol×K)].
D_p: Particle diameter, [m].
G: mass velocity on the reaction side, [Kg/(m2×s)].
n_i: molar flowrate of species i, [mol/s].
$n_i^{'}$: molar flowrate of species i, [mol/s].
P: pressure on the reaction side, [atm].
P_0: feed pressure on the reaction side, [atm].
$P^{'}$: pressure on the reaction side, [atm].
$P_0^{'}$: feed pressure on the reaction side, [atm].
R_3: external radius of the inner cylinder, [m].
T: temperature on the reaction side, [K]
T_0: feed temperature on the reaction side, [K]
$T^{'}$: temperature on the reaction side, [K]
$T_0^{'}$: feed temperature on the reaction side, [-]
u_1: inert solid profile on the reaction side, [-].
u_2: H2 flux profile on the reaction side, [mol/(m2×s)].
z: axial distance, [m].
σ_i: stoichiometric no. of component i, [-].
μ: gas viscosity on the reaction side, [Pa×s].
ε: void fraction of the reaction side, [-].
ρ: gas density on the reaction side, [Kg/m3].
$\Delta H(T)$: heat of reaction, [J/ mol].

REFERENCES

1. Shahid MZ, Farooqi AS, Fajri K, El-Adawy M, Hamdy M, Farooqi AS, Abdelaziz OY, Hossain MM, Nemitallah MA. Clean hydrogen production via sorption enhanced water gas shift reaction: A comprehensive review. Int J Hydrogen Energy 2025; 100:1483–512. https://doi.org/10.1016/J.IJHYDENE.2024.12.400
2. Kumar P, Akpan E, Ibrahim H, Aboudheir A, Idem R. Kinetics and Reactor Modeling of a High Temperature Water−Gas Shift Reaction (WGSR) for Hydrogen Production in a Packed Bed Tubular Reactor (PBTR). Ind Eng Chem Res 2008;47:4086–97. https://doi.org/10.1021/ie071547q
3. Ayastuy JL, Gutiérrez-Ortiz MA, González-Marcos JA, Aranzabal A, González-Velasco JR. Kinetics of the Low-Temperature WGS Reaction over a CuO/ZnO/Al2O3 Catalyst. Ind Eng Chem Res 2005; 44:41–50. https://doi.org/10.1021/ie049886w
4. Mendes D, Chibante V, Mendes A, Madeira LM. Determination of the Low-Temperature Water−Gas Shift Reaction Kinetics Using a Cu-Based Catalyst. Ind Eng Chem Res 2010; 49:11269–79. https://doi.org/10.1021/ie101137b
5. Saeidi S, Fazlollahi F, Najari S, Iranshahi D, Klemeš JJ, Baxter LL. Hydrogen production: Perspectives, separation with special emphasis on kinetics of WGS reaction: A state-of-the-art review. Journal of Industrial and Engineering Chemistry 2017;49:1–25. https://doi.org/10.1016/J.JIEC.2016.12.003
6. Brunetti A, Caravella A, Barbieri G, Drioli E. Simulation study of water gas shift reaction in a membrane reactor. J Memb Sci 2007;306:329–40. https://doi.org/10.1016/J.MEMSCI.2007.09.009
7. Ding OL, Chan SH. Water–gas shift reaction – A 2-D modeling approach. Int J Hydrogen Energy

2008;33:4325–36. https://doi.org/10.1016/J.IJHYDENE.2008.05.087
8. Piemonte V, De Falco M, Favetta B, Basile A. Counter-current membrane reactor for WGS process: Membrane design. Int J Hydrogen Energy 2010;35:12609–17. https://doi.org/10.1016/J.IJHYDENE.2010.07.158
9. Choi Y, Stenger HG. Water gas shift reaction kinetics and reactor modeling for fuel cell grade hydrogen. J Power Sources 2003;124:432–9. https://doi.org/10.1016/S0378-7753(03)00614-1
10. Francesconi JA, Mussati MC, Aguirre PA. Analysis of design variables for water-gas-shift reactors by model-based optimization. J Power Sources 2007;173:467–77. https://doi.org/10.1016/J.JPOWSOUR.2007.04.048.